

EMPIRICAL MODE DECOMPOSITION/ HILBERT TRANSFORM
ANALYSIS OF POSTURAL RESPONSES TO SMALL
AMPLITUDE ANTERIOR-POSTERIOR SINUSOIDAL
TRANSLATIONS OF VARYING FREQUENCIES

RAKESH PILKAR

Department of Electrical and Computer Engineering
Clarkson University, Potsdam, NY13699, USA

ERIK BOLLT

Department of Mathematics
Clarkson University, Potsdam, NY13699, USA

CHARLES ROBINSON

Department of Electrical and Computer Engineering
Clarkson University, Potsdam, NY13699, USA
Center for Rehabilitation, Science and Technology (CREST)
Clarkson University, Potsdam, NY13699, USA

(Communicated by the associate editor name)

ABSTRACT. Bursts of 2.5mm horizontal sinusoidal oscillations of sequentially varying frequencies (0.25 to 1.25 Hz) are applied to the base of support in anterior-posterior direction to study postural control. The Empirical Mode Decomposition (EMD) algorithm decomposes the Center of Pressure (CoP) data (5 young, 4 mature adults) into Intrinsic Mode Functions (IMFs). Hilbert transforms were applied to produce each IMFs time-frequency spectrum. The most dominant mode in total energy indicates a sway ramble by having its frequency content below 0.1 Hz. Other modes illustrate that the stimulus frequencies produce a ‘locked-in’ behavior of CoP with platform position signal. The combined Hilbert Spectrum of these modes shows that this phase-lock behavior of APCoP is more apparent for 0.5, 0.625, 0.75 and 1 Hz perturbation intervals. The instantaneous energy profiles of the modes depict significant energy changes during the stimulus intervals in case of lock-in. The EMD technique provides the means to visualize multiple oscillatory modes present in the APCoP signal with their time scale dependent on the signals’s successive extrema. As a result, the extracted oscillatory modes clearly show the time instances where the subject’s APCoP clearly synchronizes with the provided sinusoidal platform stimulus and where it does not.

1. Introduction. The Human postural control mechanism can be studied via various biomechanical protocols. These tests can be either static or dynamic. Providing the stimulus to the base of support and observing the reaction to these stimuli by the posture control mechanism is one of popular dynamic methods used by the researchers [16],[3],[18]. The type of stimulus used

2000 *Mathematics Subject Classification.* Primary: 92C55, 92C10; Secondary: 93C70.

Key words and phrases. Empirical Mode Decomposition, Posture and Balance, Sinusoidal Perturbations, Center of Pressure, Induced Oscillations.

This study was supported by NIH R01 AG26553, a VA Senior Rehabilitation Research Career Scientist award (CJR) and a Coulter Foundation Grant to Clarkson University.

could be of different forms as well. It can be translational or rotational. Moreover, these translational stimuli can be unidirectional as well as sinusoidal or even both. Human balance can also be studied by providing a visual perturbation [10]. The Center of Gravity (CoG) and CoP are two variables of interest for studying posture control mechanisms. For this study, we use APCoP changes collected during sinusoidally perturbed stance. Human postural control responses to sinusoidal perturbations have been studied before [1],[9]. Bugnariu et al. studied the age related changes in postural responses to externally as well as self triggered platform oscillations of 20 cm (peak-peak) with increasing frequencies up to 0.61 Hz [9]. De Nunzio et al. studied the effect of sinusoidal translations of 0.2 Hz and 0.6 Hz on balance strategies in AP directions [1]. However, the crux of our study is based on the fact that the normal postural detection and controller mechanisms are best studied by the perturbation probes that lay within the range of normal sway. Hence, for this study, the maximum stimulus amplitude is 5 mm (peak-peak) with the stimulus frequency sequentially varying from 0.25 to 1.25 Hz. Our goal is to see how the subjects' reaction to the stimulus varies with the stimulus frequency. The recognition of the presented stimulus is characterized by having the APCoP time-series profile phase-locked with the platform position signal. In other words, the frequency of sway switches from its natural value (Quiet Standing) to the presented stimulus frequency in case of a phase-lock response. To study how this particular response varies with changing stimulus frequency and time, there is a need of a reliable time-frequency representation of this signal.

The APCoP profile is characterized by the multiple frequency oscillations with different amplitudes. It is shown to be nonstationary [11]. For the nonstationary signals like these, the notion of frequency is ineffective [2]. Hence, there arises a need of a parameter which accounts for the time varying nature of the signal. This is fulfilled by the term 'instantaneous frequency'. However, this term has received both positive and negative criticisms; and in general, it has been accepted for the monocomponent signals [2],[6],[7]. Huang et. al. developed the method of EMD that decomposes the signal into IMFs involving only one mode of oscillations and no complex riding waves [8]. Hence, the notion of instantaneous frequency fits with these decomposed signals and allows us to apply the Hilbert transforms to get instantaneous frequency measures. Also, the process of sifting uses the time lapse between the successive extrema to define the time scale of the oscillatory mode [8]. This kind of decomposition not only provides a better resolution of the mode, but also gives us an opportunity to extract a mode that clearly detects the time instances as well as duration of the events where the subject's APCoP clearly synchronizes with the imparted sinusoidal platform stimulus.

On the other hand, other classical methods like the Short-Time-Fourier-Transform (STFT) or the Wigner-Ville distribution can provide only the information about the global frequency content of the signal and not about the local attributes. Also, applying these techniques on non-stationary signals like APCoP time-series have always been a topic of debate. Huang et al. have also demonstrated the advantages of EMD-Hilbert transform over these methods [8].

For this study, our approach is to decompose a subject's CoP into intrinsic mode functions and to observe 1) how these modes contribute to the subject's overall response to the sinusoid translation of the base of support, and 2) how the stimulus frequencies effect each mode. The instantaneous energy of the whole CoP time series as well as each extracted mode are studied as well. The preliminary results were submitted at [13].

2. Methods.

2.1. Subjects. Nine subjects (5 Young Adults, 4 Mature Adults) with no current or past record of peripheral neuropathy or orthopedic injury were used for this study with Clarkson University's IRB approval. Subjects underwent an informed consent procedure and preliminary testing to confirm their willingness and aptitude for participating in the study.

2.2. Data Acquisition System. A unique device, the Sliding Linear Investigative Platform For Assessing Lower Limb Stability, Simultaneous Tracking, EMG and Pressure measurement (SLIP-FALLS-STEPm), is used to provide anterior-posterior vibrations free translations. The detailed explanation of the device is given elsewhere [4]. Load cells data collected as one of the inputs to this system are used to calculate the center of pressure profiles in both the anterior-posterior and medial-lateral directions (AP and ML). A Tekscan (HR mat) pressure mat is used to validate this data. The platform position and APCoP data are collected at 1kHz, 10Hz low-pass-filtered and downsampled to 100 Hz. The subjects are blindfolded throughout the testing to block any potential visual cues and provided with aural masking noise (70 dB SPL) via headphones.

2.3. Testing Protocol. In this protocol, the platform frequency is swept in discrete steps from 0.25 Hz to 1.25 Hz (Table 1). A single trial consists of initial quiet standing (QS) period of 32 s followed by seven stimulus frequency blocks (see Table 1), each block of 32 s, and finally ending with a 32 s QS period. The table below shows the number of cycles presented in each block for each frequency. The SLIP-FALLS PMAC controller smoothes the transition from one frequency to the next [4].

Frequency (Hz)	No. of Cycles
0.25	8
0.375	12
0.5	16
0.625	20
0.75	24
1	32
1.25	40

TABLE 1. Number of cycles presented for each frequency component in a single trial

We know that human sway does not contain any appreciable energy above 2 Hz [15]. Even the presence of frequency components greater than 1.5 Hz is atypical. Also, we are interested in testing the subjects around their natural sway frequency. Soames et al. showed the presence of three modal frequencies in AP direction - primary (0.30 - 0.45 Hz), secondary (0.6 - 0.75 Hz) and tertiary (1.05 - 1.20 Hz) [15]. Hence, our stimulus frequency starts from 0.25 Hz, which is below the natural frequency but still perceivable. Then the stimulus frequency is incremented in steps every 32 s. The amplitude for the trials is set to 2.5 mm and is selected based on our experience with a previous stimulus perception study [17].

Figure 1 shows the platform position signal along with a subject's APCoP response, with frequencies varying from low to high.

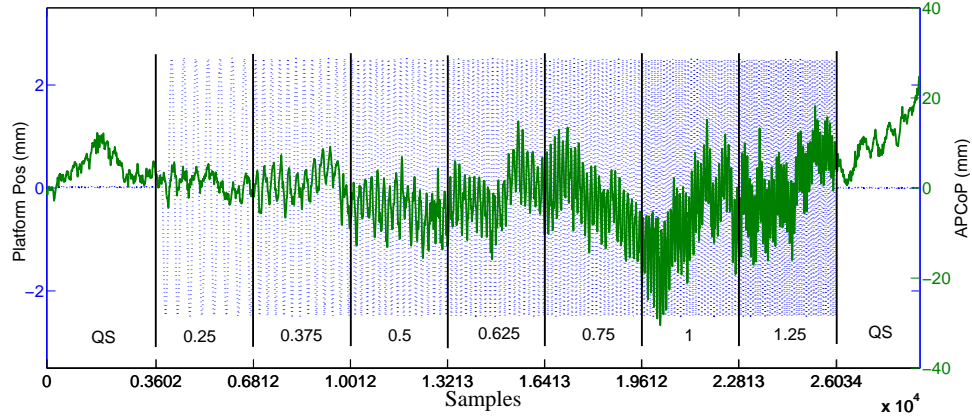


FIGURE 1. Sweep trial with platform position of 2.5mm amplitude and frequencies swept from low to high (dotted) and subject's APCoP (solid). The solid black vertical bars were added for illustration purpose only.

3. Empirical Mode Decomposition.

3.1. **EMD Algorithm.** Here we give a brief review of the method in Huang et. al to develop an EMD of a signal [8].

1. In the process, local maxima and minima of $x(t)$ are identified. The local maxima are connected by an envelope obtained by cubic spline, and the process is repeated for local minima.
2. The mean of upper and lower envelope, m_1 is subtracted from $x(t)$ to get the first component, h_1 .
3. If this component contains riding waves or asymmetry, it is treated as new data and the above process is repeated to get h_{11} . The process is again repeated till we get h_{1k} as the first IMF, c_1 .

$$h_{1(k-1)} - m_{1k} = h_{1k} = c_1 \quad (1)$$

4. The extracted IMF c_1 is then subtracted from the original data and the process is repeated on the residual to get the second IMF, and so on.
5. However, excessive application of this process can result into IMF which could be a pure frequency modulated signal of constant amplitude. Hence, the limitation on the standard deviation calculated from two consecutive sifting processes is used as a stopping criterion.

$$0.2 \leq \sum_{t=0}^T \left[\frac{|h_{1(k-1)}(t) - h_{1k}(t)|^2}{h_{1(k-1)}^2(t)} \right] \leq 0.3 \quad (2)$$

6. Thus the sifting process allows the signal $x(t)$ to be decomposed into n IMFs with final residual r_n .

3.2. **Hilbert Spectrum.** Once all the IMFs and final residual are extracted from the data, a Hilbert transform [8],[5], is applied to each IMF. The final residual, r_n is either a monotonic function or a constant, and hence it can be removed.

$$\begin{aligned} HT \{IMF_1\} &= a_1(t) e^{i \int \omega_1(t) dt} \\ HT \{IMF_2\} &= a_2(t) e^{i \int \omega_2(t) dt} \\ &\vdots \\ &\vdots \\ HT \{IMF_n\} &= a_n(t) e^{i \int \omega_n(t) dt} \end{aligned} \quad (3)$$

3.3. **Instantaneous Energy.** For time discrete signals, the energy of a signal, E_d , is defined as the sum of the squared magnitude of the samples. Hence, the instantaneous energy of a signal $x(t)$ is calculated as:

$$E_i(t) = \int_{t-\tau}^t x^2(t) dt \quad (4)$$

Note that the term ‘energy’ does not refer to the concept of conservation of energy. The instantaneous value of the energy represents the size of the signal in this situation. This energy operator was applied on every IMF extracted as well as on the original data.

4. Results.

4.1. Platform Position Data. The EMD-HT algorithm is first applied on the platform position signal because its frequency content is known. The position mode 1 and its Hilbert transform spectrum faithfully track the oscillation frequency (Figure 3).

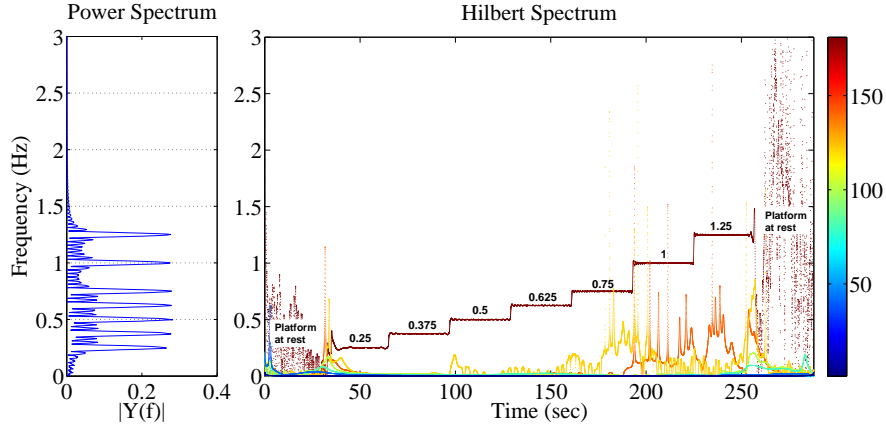


FIGURE 2. The Power Spectrum using DFT(Left) and the Hilbert spectrum obtained by applying the EMD algorithm (Right) on the platform position signal

4.2. APCoP Data. The algorithm can be now applied to the APCoP data collected during the same trial (Figure 3). The EMD method decomposes the signal into 10 IMFs, as shown in Figure 4. For the APCoP, the Hilbert spectrum shows that the most dominant mode in total energy has its

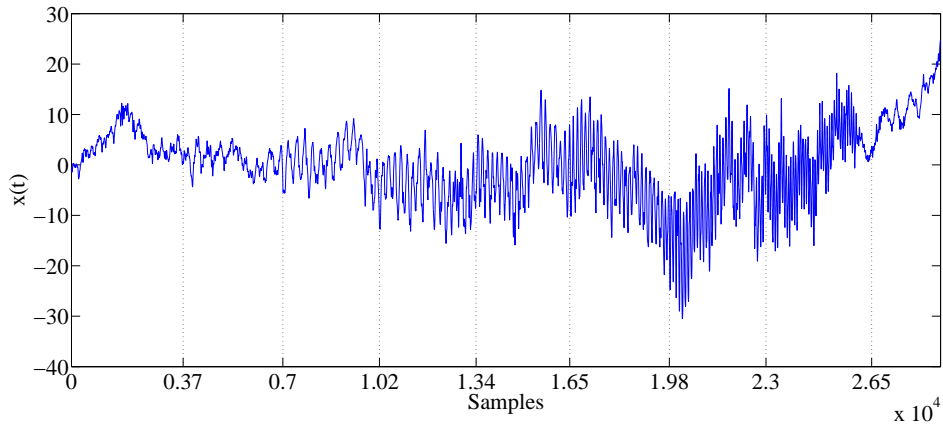


FIGURE 3. The APCoP response collected during a sweep trial from 20 y.o. female subject

frequency content below 0.1 Hz, thus indicating a sway ramble or a low frequency drift present in the sway. Other modes in turn illustrate that the stimulus frequencies produce a ‘lock-in’ behavior of CoP with platform position oscillation. This lock-in response is seen in several modes partially, and not in a single mode as a frequency modulated signal. Also, this locked-in behavior is more

apparent for 0.5, 0.625, 0.75 and 1 Hz perturbations, possibly because of the limited number of cycles presented at 0.25 and 0.375 (Table 1).

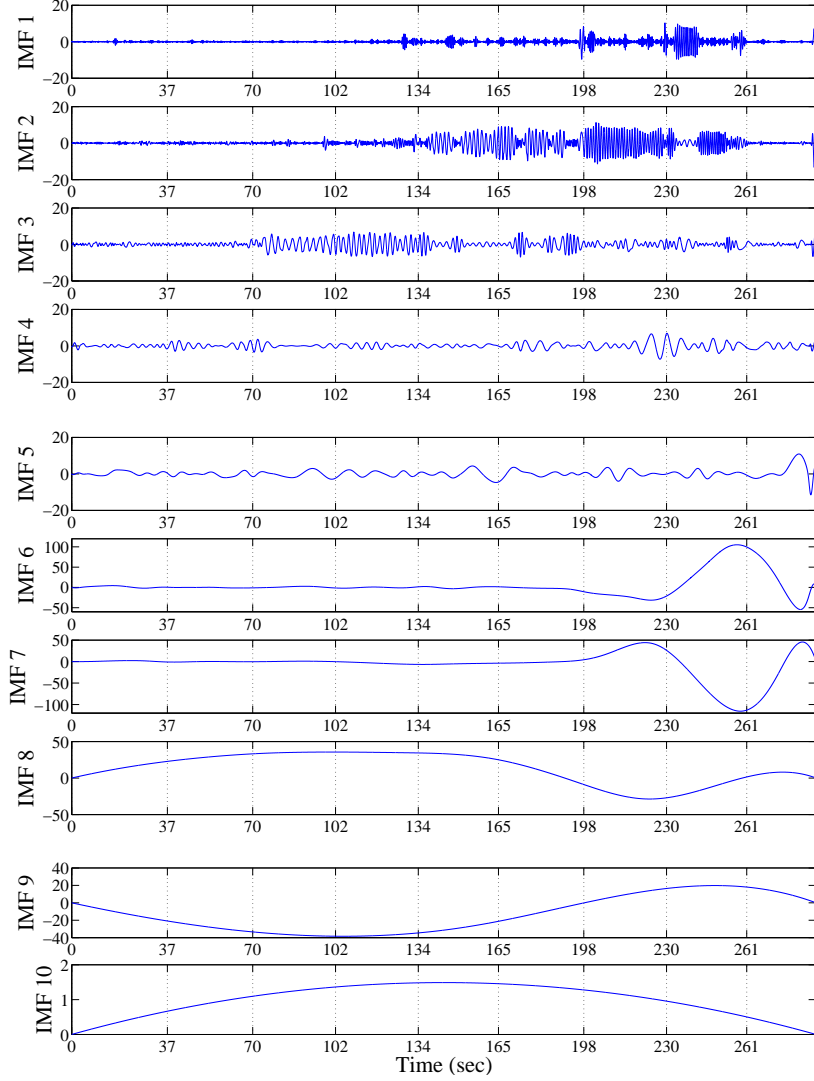


FIGURE 4. The ten IMFs extracted from the APCoP time series by the EMD method

The EMD algorithm decomposes the APCoP signal into ten intrinsic mode functions (Figure 5). The Hilbert transforms of these individual modes and their instantaneous energy profiles reveal more information. The individual modes track the frequencies from their high to lower order. The first mode (IMF 1) shows 1.25 and 1 Hz components, while the last one showing the lowest frequency reactions. Point-by-point summation of all of these modes with the final residual yields back the test signal with mean error of -1.7×10^{-17} ensuring the “completeness” of the EMD algorithm. For the test signal shown in Figure 4, the Hilbert spectra and the instantaneous energy plots of IMF 1 to IMF 4 are shown in Figure 5 to Figure 8, respectively.

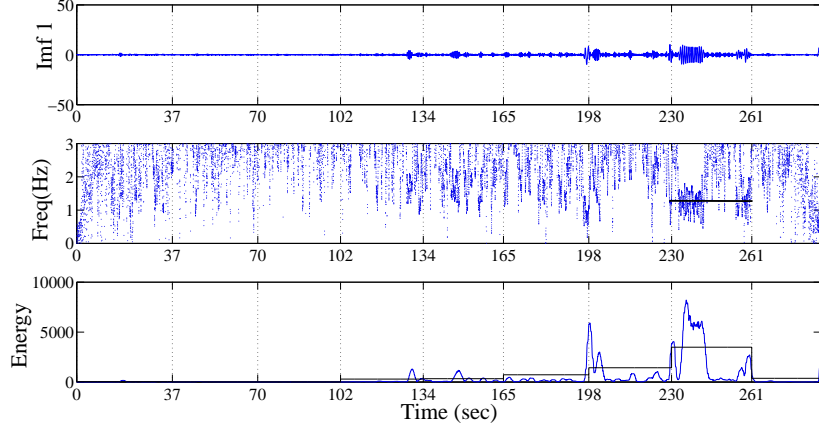


FIGURE 5. IMF 1 (top), its Hilbert spectrum (center) and instantaneous energy (bottom). Horizontal lines are added for reference

As shown by the Hilbert spectrum in Figure 5, the first IMF tracks the highest frequency component present in the signal. It is also the one of the stimulus frequencies, and it presented during the 230 s to 261 s time interval. The instantaneous energy plot shown above also verifies this by showing the significant energy content during the period of lock-in. A phase-locked response is present for approximately half of the stimulus interval for this mode, and the rest of the response is observed in the Hilbert spectrum of IMF 2 shown in Figure 6.

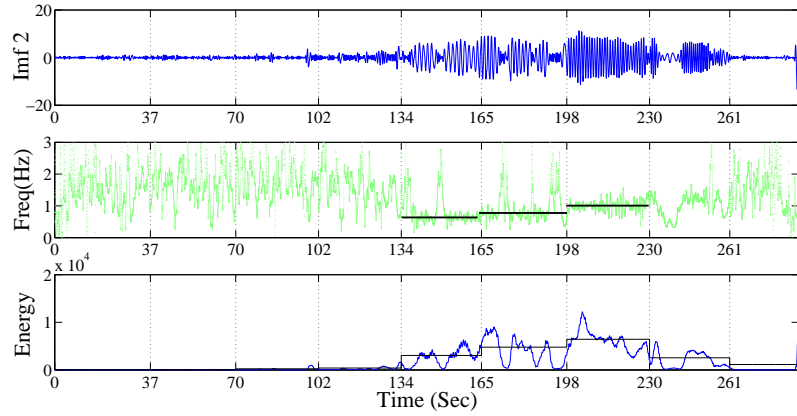


FIGURE 6. IMF 2 (top), its Hilbert spectrum (center) and instantaneous energy (bottom)

Now, the algorithm moves to the lower frequencies, this time tracking 0.625 Hz, 0.75 Hz, 1 Hz and the remaining portion of 1.25 Hz (shown by horizontal solid lines in the Hilbert spectrum). Also, the energy during these stimuli intervals was significantly higher than the other stimuli intervals.

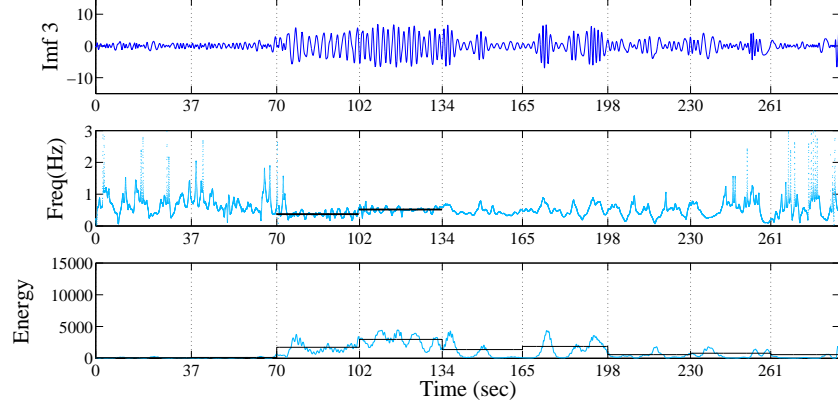


FIGURE 7. IMF 3 (top), its Hilbert spectrum (center) and instantaneous energy (bottom)

Similarly, IMF 3 detects the lower frequencies, 0.375 Hz and 0.5 Hz that are present in the APCoP signal. The higher energy shown during these intervals is plotted in Figure 7(bottom).

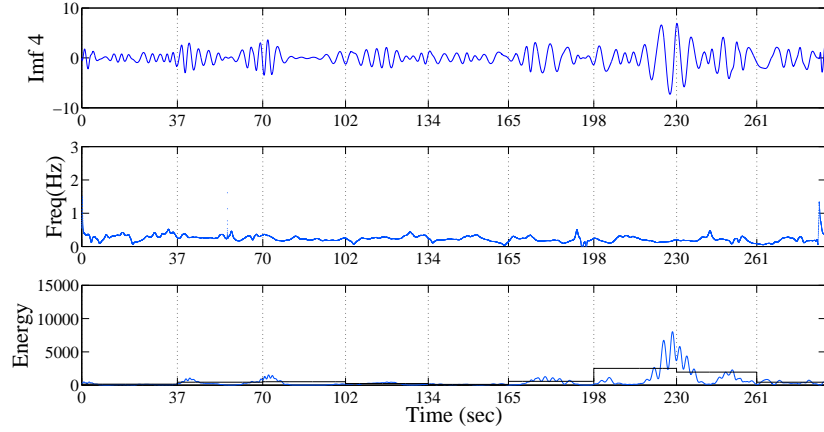


FIGURE 8. IMF 4 (top), its Hilbert spectrum (center) and instantaneous energy (bottom)

The Hilbert Spectrum of IMF 4 shows a monotonic response (Figure 9 middle). The instantaneous frequency for this mode is found to be around 0.25 Hz and does not show any significant variation during the complete trial.

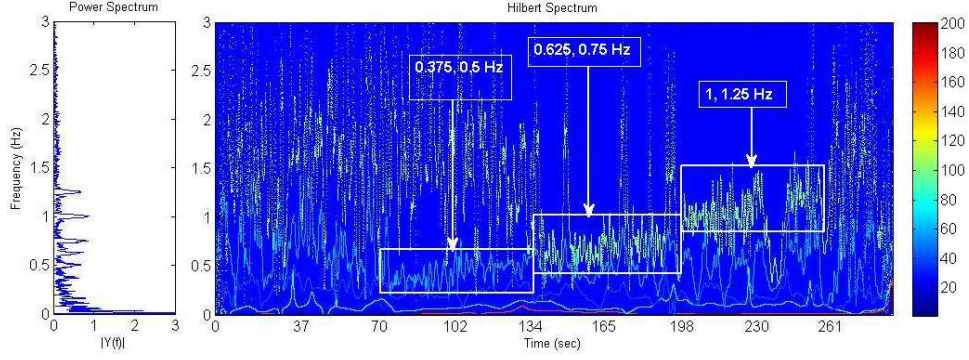


FIGURE 9. The combined Hilbert Spectrum with the colorbar (right) and the Discrete Fourier transform (left) of the APCoP data collected during a Sweep trial

The contribution of all these modes extracted can be studied by merging all their Hilbert spectra (Figure 9). As the frequencies detected by individual modes overlap, it reveals the regions where the phase-lock behavior of the APCoP is more apparent. Thus, for the stimulus whose frequencies are sequentially increased from 0.25 Hz to 1.25 Hz, the subject's lock-in response is more apparent at frequencies from 0.625 Hz to 1 Hz. The color bar indicates that intensity level or the energies (obtained by EMD-HT) during these regions are higher than the one at the low frequency regions.

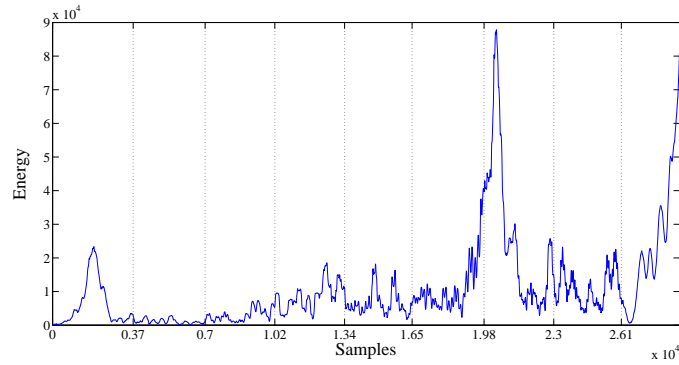


FIGURE 10. The instantaneous energy of the APCoP signal according to Equation 5

Figure 10 shows the result of applying this energy operator on the APCoP time series shown in Figure 3. The instantaneous energy value reaches maximum (with some latency) when the platform switches from 0.75 Hz to 1 Hz. The value is smaller for 0.25 Hz (37-70 sec) and 0.375 Hz (70-102 sec) intervals as compared with other higher frequency intervals.

Next, we consider the root-mean-square value of the instantaneous energy during each stimulus interval (interval 1 to 7 for 0.25 to 1.25 Hz) trial. It is calculated for every subject and is compared between the matured and young adult groups.

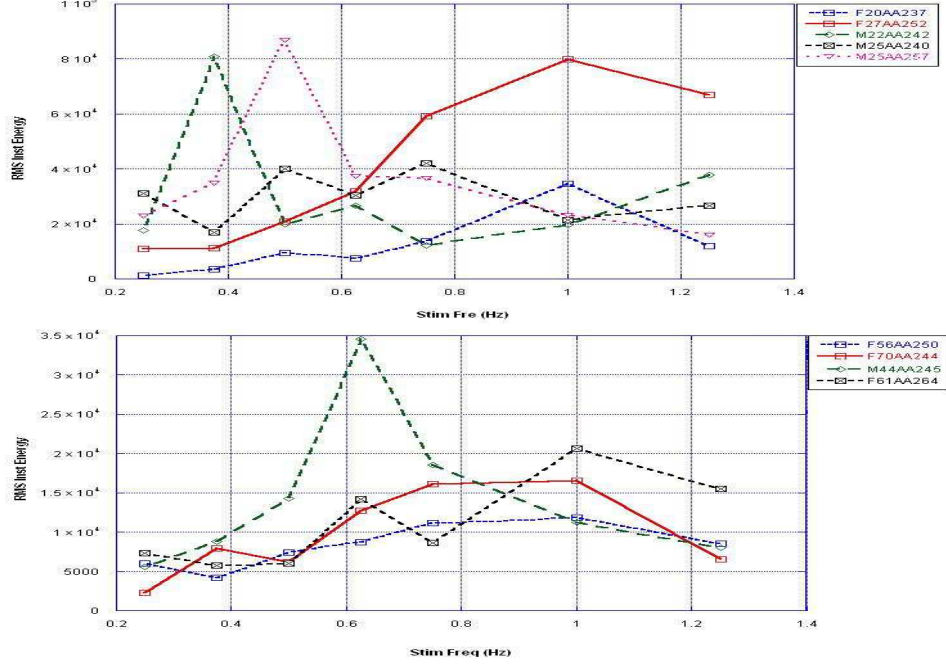


FIGURE 11. The rms values of instantaneous energy of the APCoP signal during each stimulus interval according to Equation 5, for (top) young adults, (bottom) for healthy mature adults

For two young adults (M22AA242 and M25AA257), the instantaneous energy rms is found to be higher at 0.375 Hz and 0.5 Hz, respectively. Two other young adults, F27AA252 and F20AA237, show an increase in the instantaneous energy with an increase in the stimulus frequency until 1 Hz interval (Interval 6).

For the mature adults, the energy values for the lower frequency intervals (Interval 1 and 2 for 0.25 Hz and 0.375 Hz respectively) are smaller than the rest. M44AA245 clearly shows the maximum response at 0.625 Hz.

5. Discussion. Our approach is based on the fact that the normal postural detection and controller mechanisms are best studied by the perturbation probes that lay within the range of normal sway. Bugnariu et al. used the platform oscillations of 20 cm (peak-peak) for their study which are much higher than any normal healthy subject's natural CoP range. The testing frequencies were less than 0.7 Hz for both Bugnariu et al and De Nunzio et al. [1],[9]. The wide range of stimulus frequencies in our study provides us an opportunity to observe the postural control responses below, at, and above their natural sway frequency in a single trial with the stimulus amplitude kept well below the natural CoP sway range. Providing a stimulus of considerably higher amplitudes can not only make the subject take extreme actions to gain necessary balance control, but can also affect them psychologically for the rest of the testing process. By providing translations of 5mm (peak-peak) amplitude, we ensure that they always lie within the natural sway range of a healthy person.

The idea behind using the EMD algorithm to decompose the APCoP signal into the intrinsic mode functions is to represent the oscillation modes imbedded in the signal. The IMF each cycle is defined by zero crossings, and involves only one mode of oscillation, removing the complex riding waves [8]. Moreover, the process of sifting uses the time lapse between the successive extrema as the definition of the time scale for the intrinsic oscillatory mode [8]. This approach not only makes the algorithm applicable to the signals with a non-zero mean but also provides for the better resolution of the oscillatory modes. The idea of IMFs and process of decomposition perfectly fit our need for analyzing the APCoP data collected in response to sinusoidal translations of time

varying frequency. Using the method of sifting, we are more likely to detect the time instances of two particular scenarios. One when subject responds to the stimulus by locking to the platform position signal; and second, when the stimulus frequency is either too fast to too slow to be tracked by the subject's APCoP.

Also, given the nature of our experiment, most subjects sway at a particular stimulus frequency and switch to the next frequency when the next interval starts. This 'switching' can be easily seen in one of the extracted modes and its instantaneous frequency, thus making EMD-HT extremely suitable for the analysis. As a confirmation, the instantaneous energy plots of each IMF also showed significant changes during the lock-in intervals.

Sparto et al. provided sinusoidal perturbations to the visual sensory system and proposed the method to determine if the postural response was present using F-statistics [12]. In their study, they used sinusoidal optical flow at 0.1 Hz and 0.25 Hz and quantitatively showed if the response was present or not [12]. Although, the EMD algorithm is another approach to qualitatively determine the presence of response at given broad range of frequencies, the instantaneous energy operator provides the quantitative measures of the subjects' responses in terms of the rms value of the instantaneous energy during each stimulus frequency interval. The ability of EMD to access these local oscillations allows us to understand the range of frequencies at which a subject's lock-in behavior is more apparent. The modes and their Hilbert spectrum clearly demonstrated how subjects' responses shifted from one frequency interval to the other.

6. Conclusion. The basic EMD-HT method provides the means to dissect an APCoP time-series signal into multiple oscillatory modes, and allows us to observe the contribution of these modes to a subject's overall response to the sinusoidal oscillations of the base of support. For APCoP, the mode that was most dominant in total energy had its frequency content below 0.1 Hz, thus indicating a sway ramble. Other modes detected the induced oscillations in APCoP and showed that the stimulus frequencies produced a 'lock-in' behavior between CoP and platform position oscillation. The combined time-frequency representation of these modes showed that this phase-lock behavior of APCoP was more apparent for the 0.5, 0.625, 0.75 and 1 Hz perturbation intervals for all the young adult subjects. This was also confirmed by the instantaneous energy plots. The instantaneous energy plots for the mature adults had monotonous response for all the stimuli intervals except for one 44 y.o. mature adult who had the highest response at 0.625 Hz. The visual assessment of all the results was done by observing the Hilbert spectra of all the APCoP responses.

Acknowledgements. The authors would also like to thank Xiaoxi Dong and Anne Launt for providing the experimental data for this study.

REFERENCES

- [1] AM Nunzio, A. Nardone and M. Schieppati, *Head stabilization on a continuously oscillating platform: the effect of proprioceptive disturbance on the balance strategy*, Experimental Brain Research, **165**(1) (2005), 261–272.
- [2] B. Boashash, *Estimating and Interpreting the Instantaneous Frequency of a Signal - Part 1: Fundamentals*, Proceedings of the IEEE, **80**(4) (1992), 520–538.
- [3] C. Tokuno, A. Cresswell, A. Thorstensson and M. Carpenter, *Age-related changes in postural responses revealed by support-surface translations with a long acceleration-deceleration interval*, Clinical Neurophysiology, **121** (2010), 109–117.
- [4] C. Robinson, M. Purucker and L. Faulkner, *Design, Control and Characterization of a Sliding Linear Investigative Platform for Analyzing Lower Limb Stability (SLIP-FALLS)*, IEEE Transactions on Rehabilitation Engineering, **6**(3) (1998), 334–350.
- [5] F. King, "Encyclopedia of Mathematics and its Applications - Hilbert Transforms", Volume 1, Cambridge University Press, New York, 2009.
- [6] L. Cohen, *Time Frequency Distributions - Review*, IEEE Transactions on Neural Systems and Rehabilitation Engineering, **77**(7) (2002), 941–981.
- [7] L. Cohen and C. Lee, *Instantaneous frequency, its standard deviation and multicomponent Signals*, Advanced Algorithms and Architectures for Signal Processing III, Franklin T. Luk, Ed., Proc. SPIE, **975** (1988), 186–208.
- [8] N. Huang, Z. Shen, S. Long, M. Wu, H. Shih, Q. Zheng, N. Yen, C. Tung and H. Liu, *The empirical mode decomposition and the Hilbert spectrum for nonlinear and non-stationary time series analysis*, Proc. Royal Society London A, **454** (1998), 903–995.

- [9] N. Bugnariu and H. Sveistrup, *Age-related changes in postural responses to externally- and self-triggered continuous perturbations*, Archives of Gerontology and Geriatrics, **42** (2006), 73–89.
- [10] P. Loughlin and M. Redfern, *Spectral Characteristics of Visually Induced Postural Sway in Healthy Elderly and Healthy Young Subjects*, IEEE Transactions on Neural Systems and Rehabilitation Engineering, **9**(1) (2001), 24–30.
- [11] P. Loughlin, M. Redfern and J. Furman, *Nonstationarities pf Postural Sway*, IEEE Engineering in Medicine and Biology Magazine, **22**(2) (1998), 69–75.
- [12] P. Sparto, J. Jasko and P. Loughlin, *Detecting postural responses to sinusoidal sensory inputs: A Statistical Approach*, IEEE Transactions on Neural Systems and Rehabilitation Engineering, **12**(3) (2004), 360–366.
- [13] R. Pilkar, E. Boltt and C. Robinson, *Empirical Mode Decomposition/ Hilbert Transform Analysis of Induced Postural Oscillations*, BMES Annual Meeting,(2010).
- [14] R. Schilling and C. Robinson, *A phase-locked looped model of the response of the control system to periodic platform motion*, IEEE Transactions on Neural Systems and Rehabilitation Engineering, **18**(3) (2010), 274–283.
- [15] R. Soames and J. Atha, *The Spectral characteristics of postural sway*, European Journal of Applied Physiology and Occupational Physiology, **49**(2) (1982), 169–177.
- [16] S. Richerson, L. Faulkner, C. Robinson, M. Redfern and M. Purucker, *Acceleration Threshold Detection During Short Anterior and Posterior Perturbations on a Translating Platform*, Gait and Posture, **18** (2003), 11–19.
- [17] S. Nakappan, C. Robinson, V. Dharbe, C. Storey and K. O’Neal, *Variations in Anterior - Posterior COP patterns in elderly adults between psychophysically detected and non-detected short horizontal perturbations*, IEEE-EMBS 27th Annual International Conference, (2005), 5427–5430.
- [18] V. Dietz, M. Trippel, I. Ibrahim and W. Berger, *Human Stance on a Sinusoidally Translating Platform: Balance Control by Feedforward and Feedback Mechanisms*, Experimental Brain Research, **93** (1993), 352–362.

Received September 17, 2010; Accepted February 00, 2010.

E-mail address: robinson@clarkson.edu

E-mail address: pilkarrb@clarkson.edu

E-mail address: boltttem@clarkson.edu